

---

This is an electronic reprint of the original article.  
This reprint may differ from the original in pagination and typographic detail.

Noor, Imtisal e.; Martin, Andrew; Dahl, Olli

**Water recovery from flue gas condensate in municipal solid waste fired cogeneration plants using membrane distillation**

*Published in:*  
Chemical Engineering Journal

*DOI:*  
[10.1016/j.cej.2020.125707](https://doi.org/10.1016/j.cej.2020.125707)

Published: 01/11/2020

*Document Version*  
Publisher's PDF, also known as Version of record

*Published under the following license:*  
CC BY

*Please cite the original version:*  
Noor, I. E., Martin, A., & Dahl, O. (2020). Water recovery from flue gas condensate in municipal solid waste fired cogeneration plants using membrane distillation. *Chemical Engineering Journal*, 399, Article 125707. <https://doi.org/10.1016/j.cej.2020.125707>

---

This material is protected by copyright and other intellectual property rights, and duplication or sale of all or part of any of the repository collections is not permitted, except that material may be duplicated by you for your research use or educational purposes in electronic or print form. You must obtain permission for any other use. Electronic or print copies may not be offered, whether for sale or otherwise to anyone who is not an authorised user.



# Water recovery from flue gas condensate in municipal solid waste fired cogeneration plants using membrane distillation

Imtisal-e- Noor<sup>a,b,\*</sup>, Andrew Martin<sup>a</sup>, Olli Dahl<sup>b</sup>

<sup>a</sup> Department of Energy Technology, KTH Royal Institute of Technology, Stockholm, Sweden

<sup>b</sup> Department of Bioproducts and Biosystems, Aalto University, Espoo, Finland

## HIGHLIGHTS

- Performance of proposed MD process is better than that of existing RO process.
- Ammonia removal efficiency was enhanced by pH adjustment.
- 92% water was recovered from real flue gas condensate during reconcentration study.
- Clean condensate cost: 1.7 \$/m<sup>3</sup> for district heating driven MD system.

## ARTICLE INFO

### Keywords:

Energy analysis  
Flue gas condensate  
Membrane distillation  
Process economy  
Separation efficiency  
Sustainable development goals

## ABSTRACT

In cogeneration plants with wet scrubbing of exhaust gases, the resulting flue gas condensate passes through various treatment steps prior to its discharge to recipient water body or for use as boiler feed water. The present investigation examines membrane distillation (MD) as an alternative treatment method, potentially overcoming bio-fouling and other known drawbacks of established membrane technologies while making efficient use of available heat sources and sinks. Laboratory and pilot scale experiments are performed using air gap MD system where acid neutralization has been considered as a pretreatment step in order to avoid ammonia slip. Separation efficiency, transmembrane flux, specific heat demand and net heat demand were determined at different operating conditions. Resultant separation efficiency of the contaminants shows the successful application of MD for flue gas condensate treatment, achieving results that are comparable or even better than separation with reverse osmosis (RO). The obtained transmembrane flux varied between 1.6 and 7.2 L/m<sup>2</sup>h per module depending upon the hot and cold side temperatures. For various operating conditions, specific heat demand ranged from 400 to 1000 kWh/m<sup>3</sup> per module and corresponding net heat demand was around 17.5–110 kWh/m<sup>3</sup>. The reconcentration study found that 92% of water could be recovered from the tested flue gas condensate. Process economy shows that estimated clean condensate production cost can be as low as 1.7 \$/m<sup>3</sup>.

## 1. Introduction

Strict environmental regulations embodied in UN sustainable development goals 9 (Industry, Innovation, and Infrastructure) and 12 (Responsible Consumption & Production) imply use of advanced pollution controls in combined heat and power plants (CHPs) in order to minimize emissions of particulates, heavy metals, acid gases, organochlorides (dioxins), and nitrogen oxides [1]. Wet scrubbing is often employed, and the high dew points encountered in the flue gas condensation system allow for thermal energy recovery for district heating (DH) or local heating along with water recovery [2]. The resulting flue gas condensate contains an aqueous mixture (30–55% water content by

mass [3]) of acids, salts, heavy metals, and various particulate solids. Various wastewater treatment methods are applied to flue gas condensate, depending upon the overall water balance and expected end use of the treated flue gas condensate [4]. Solids and particulate removal from flue gas condensate usually involves filter bags, lamella clarifiers and sand filters. Ion exchange can be employed for separating salts and heavy metals [5]. In certain circumstances these methods are sufficient when the treated condensate is to be discharged to the recipient water body. However, in cases where levels of certain contaminants are high or where water recovery is desired for providing boiler make-up water, membrane separation techniques are preferred owing to their better efficiency and reasonable cost. For this purpose a

\* Corresponding author.

E-mail address: [ieno@kth.se](mailto:ieno@kth.se) (I.-e.- Noor).

<https://doi.org/10.1016/j.cej.2020.125707>

Received 1 April 2020; Received in revised form 26 May 2020; Accepted 28 May 2020

Available online 04 June 2020

1385-8947/ © 2020 The Author(s). Published by Elsevier B.V. This is an open access article under the CC BY license (<http://creativecommons.org/licenses/by/4.0/>).

series of treatment steps is employed [6,7], e.g. microfiltration (MF) for removing large particles and colloids, ultrafiltration (UF) for separating small particles and remaining colloids, and reverse osmosis (RO) for separating water molecules from ions.

Although RO is a well developed technology with broad acceptance in industry, there are several fundamental drawbacks that are yet to be overcome [5]. For instance, RO has a relatively high electrical energy demand for providing necessarily high intake pressures, effecting membrane performance efficiency over time. Moreover, RO is associated with pretreatment using harsh chemicals for countering biofouling on the membrane surface. Additionally, certain high-concentration feedstocks cannot be easily treated by RO owing to practical limitations, namely restrictions in upper pressurization limits. There is also a need to reduce sludge volumes by enhancing water recovery in order to solve sludge disposal issues. Therefore, novel membrane separation techniques are of high interest which have advantages of the proven methods along with high recovery ratios, reduced electrical energy demand, less sensitivity to bio-fouling, lower pretreatment and sludge disposal requirements, and ease in implementation.

In this framework membrane distillation (MD) is a promising technology that theoretically allows only volatiles (i.e., water vapor) to pass through a microporous, hydrophobic membrane [8]. MD is a thermally driven process that induces a vapor pressure difference across the membrane to direct water vapor to transfer from hot side to cold side. MD is typically capable of achieving complete rejection of non-volatile contaminants (i.e. ions, metals, macromolecules, colloids and cells). It usually operates in the range of 50–90 °C (lower operating temperatures compared to conventional distillation) and at atmospheric pressure (much lower operating pressure as compared to RO based processes) [9–11]. Moreover, its separation efficiency is relatively insensitive to concentration and pH levels. Additionally, MD has other potential benefits as compared to RO in that it can achieve higher recovery ratios, has reduced fouling issues, and involves low mechanical stress owing to low operating pressures [12,13]. These properties ensure higher permeate yield which in turn lessens fresh water demand and reduced concentrate/sludge disposal requirements, resulting in potentially lower capital investments and/or operating and maintenance costs. Furthermore, heat sources and sinks required for effective operation of MD technology are ideally suited for CHP integration.

Considering these attributes, three preliminary studies have been performed in order to examine the potential of MD for flue gas condensate treatment and water recovery: In 2004 Värmeforsk commissioned a prestudy to investigate MD technology in the CHP context [14], and a pilot unit was installed at the Vattenfall Idbäcken (biofuel-fired) CHP facility during 2006–2007 [15,16]. Results showed that particles and heavy metals in flue gas condensate were removed successfully, however, ammonium could not be separated fully, pointing to the need for future studies to address this point. Later, in 2011 a pilot unit was installed at Hammarby Sjöstadverket with testing conducted during 2012–2013 in the framework of a collaborative project between IVL Swedish Environmental Institute, Xzero AB, and KTH Royal Institute of Technology [17]. Preliminary testing of flue gas condensate obtained from Bristaverket (bio-fuel fired) CHP facility was conducted [17]. Problems with ammonium separation were again observed as in the Idbäcken trials, although separation of non-volatiles was excellent.

Since ammonium removal from flue gas condensate is crucial prior to its discharge to recipient or in reuse as CHP process water, it needs to be addressed along with removal of non-volatiles. Goldschmidt et al. [18] investigated four commercially employed alternatives for ammonium management in flue gas condensate: 1) acid quenching; 2) RO-based flue gas condensate treatment; 3) selective catalytic reduction (SCR); and 4) membrane-based ammonia strippers. The results demonstrated good ammonia removal performance in all cases, and acid quenching was judged to be the best choice owing to its lower maintenance requirements. In 2014 an acid stream quench system was installed at Bristaverket (biofuel-fired) CHP facility and showed

satisfactory performance, although biofouling in the flue gas condensate treatment process led to shorter RO membrane lifetime [19]. Other issues include inadequate separation of mercury and boron.

The combination of acid stream quench with MD represents a novel configuration, exploiting the advantages of both technologies for innovative flue gas condensate treatment. This combination can lead to improved performance as compared to RO-based alternatives: higher separation efficiency, enabling purer process water; higher concentration levels in retentate, reducing operating and maintenance (O&M) costs and capital investment of downstream equipment; minimization of biofouling, reducing O&M costs in upstream equipment; and reduced internal electricity demand. The present study is thus conducted in order to explore this novel concept in detail, based on experimental studies of MD separation for actual flue gas condensate feeds from Högdalen CHP facility. In this work, the main emphasis is on separation efficiency of contaminants and water recovery. Moreover, the effect of parametric variation on clean condensate flux and specific energy demand is examined in detail.

## 2. Högdalen CHP plant

The Högdalen CHP facility, owned by Stockholm Exergi AB, is located south of the city and employs six boilers: B1-B4 utilize municipal solid waste and collectively supplies 190 MW heating power, B5 uses biofuel and is able to supply 80 MW heating power, and the fuel source for B6 is returned waste and supplies 91 MW heating power. The process overview of Högdalen CHP plant [20] is shown in Fig. 1. The flue gas produced after incineration is sent for cleaning in order to meet appropriate environmental standards and regulations:

- Flue gas streams from boilers B1-B3 and B6 pass through a bag house after addition of ammonia (binds  $\text{NO}_x$ ), activated carbon (binds dioxins and furans) and caustic lime (binds HCl and  $\text{SO}_2$ ). The stream then goes to the two stage scrubber where at first it is acid quenched to  $\text{pH} = 1$ , and thereafter heavy metals, salts, and acids are removed. Subsequently the stream is treated with sodium hydroxide (NaOH) neutralization for removal of sulfur dioxide ( $\text{SO}_2$ ). In the next stage, flue gas condensate is produced by cooling down the flue gas to below its dew point (more on condensate treatment in subsequent sections).
- The flue gas stream from B4 is first treated by an electrostatic precipitator (ESP1) for removal of larger particles, followed by limestone scrubbing (SC1) for removal of acids (HCl and HF), ammonia, heavy metals, and other particulates. The second scrubber (SC2) treats sulfur dioxide, dioxins and furans via addition of sodium hydroxide and activated carbon. The scrubbed flue gas is then sent to the condenser for further treatment. The polluted water (contaminated with heavy metals) coming from the two scrubbers and condenser is sent to the neutralization tank to reach up to  $\text{pH} = 7$  which is further dried, passes through the electrostatic precipitator (ESP2) and added back to the stream coming from the ESP1 to send it to SC1.
- Flue gas from B5 is directly released into environment without any further cleaning.

Typically, the resulting flue gas condensate stream is heavily contaminated and needs to be treated. The overall water balance is positive since the flue gas is brought below the dew point, and surplus water can be returned to the process (thus saving fresh water purchases) or released to the recipient. The dual purpose of meeting boiler water quality standards and fulfilling wastewater restrictions points to the requirement for advanced wastewater treatment. In this setting the flue gas condensate from the condensers are firstly buffered and then passed through vibrating screens in order to remove suspended solids. The pH along with ammonia and suspended solids concentrations are measured at this point before entering into next buffer tank. Thereafter two

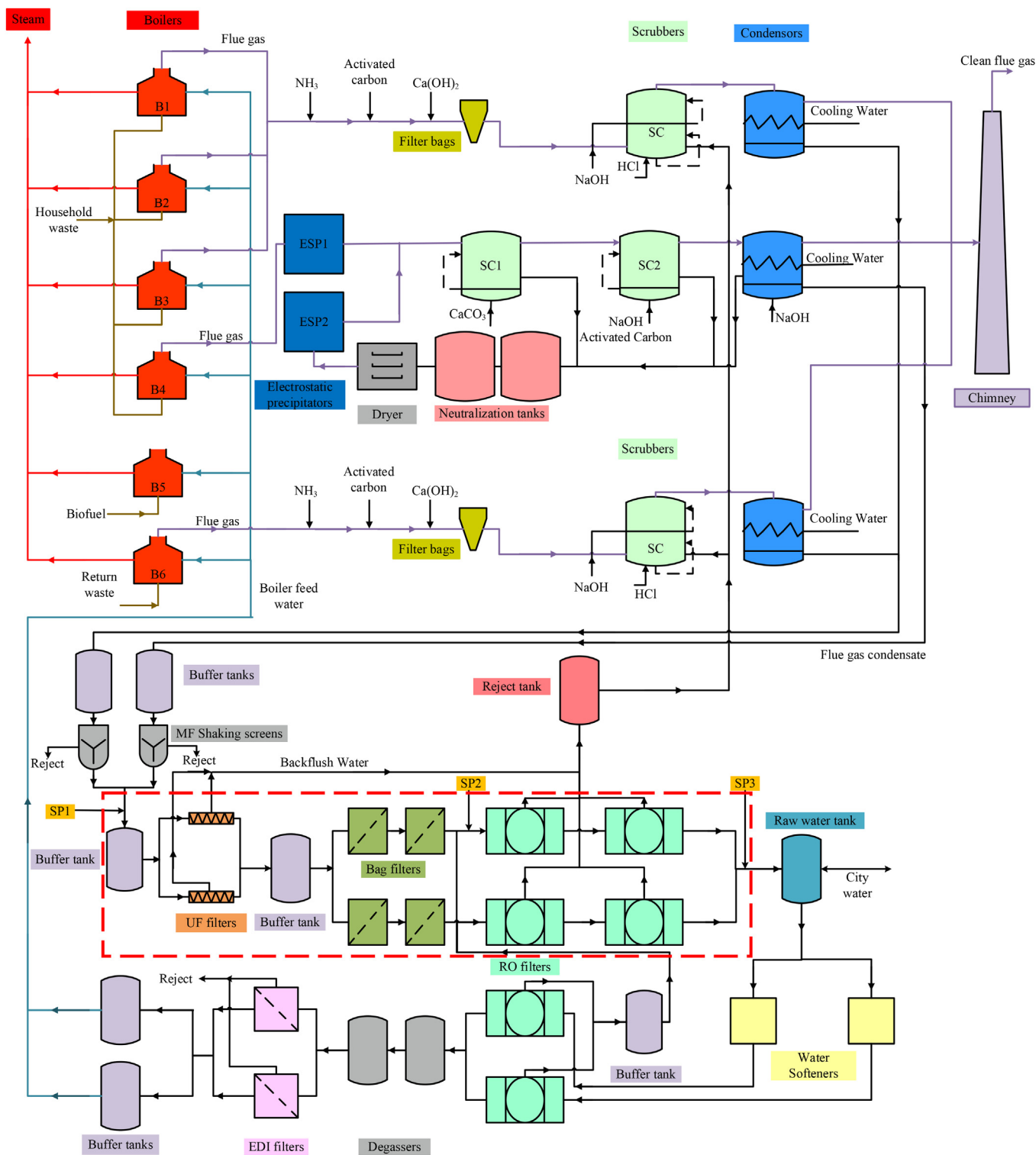


Fig. 1. Flow Diagram of Stockholm Exergi Högaldalen CHP facility where SP1, SP2 and SP3 show the sampling points. Red dashed line shows area of interest for introducing an MD system. (For interpretation of the references to colour in this figure legend, the reader is referred to the web version of this article.)

parallel streams of volumetric flowrates 45–50 m<sup>3</sup>/h are introduced to UF modules in order to remove small particulates, oils and resins (to reduce COD). This ultra-filtered flue gas condensate is then fed again into another buffer tank and afterwards is passed through bag filters for additional treatment. At this point, RO modules are installed for advanced cleaning of the flue gas condensate. The reject from the UF and RO modules is collected and returned to the scrubbers. The flowrate of RO-treated flue gas condensate is between 10 m<sup>3</sup>/h to 100 m<sup>3</sup>/h

depending upon the seasonally dependent DH requirement. After measuring the pH, ammonia, suspended solids, metals, flowrate and temperature, the RO-treated flue gas condensate (conductivity 10–20 μS/cm) is normally mixed with city water (conductivity 220 μS/cm) in the raw water tank (further referred as mixed water) in order to fulfill boiler water requirements. The mixed water is firstly treated with water softener and then introduced into the RO modules as the advanced demineralization step. The RO-treated mixed water is usually saturated

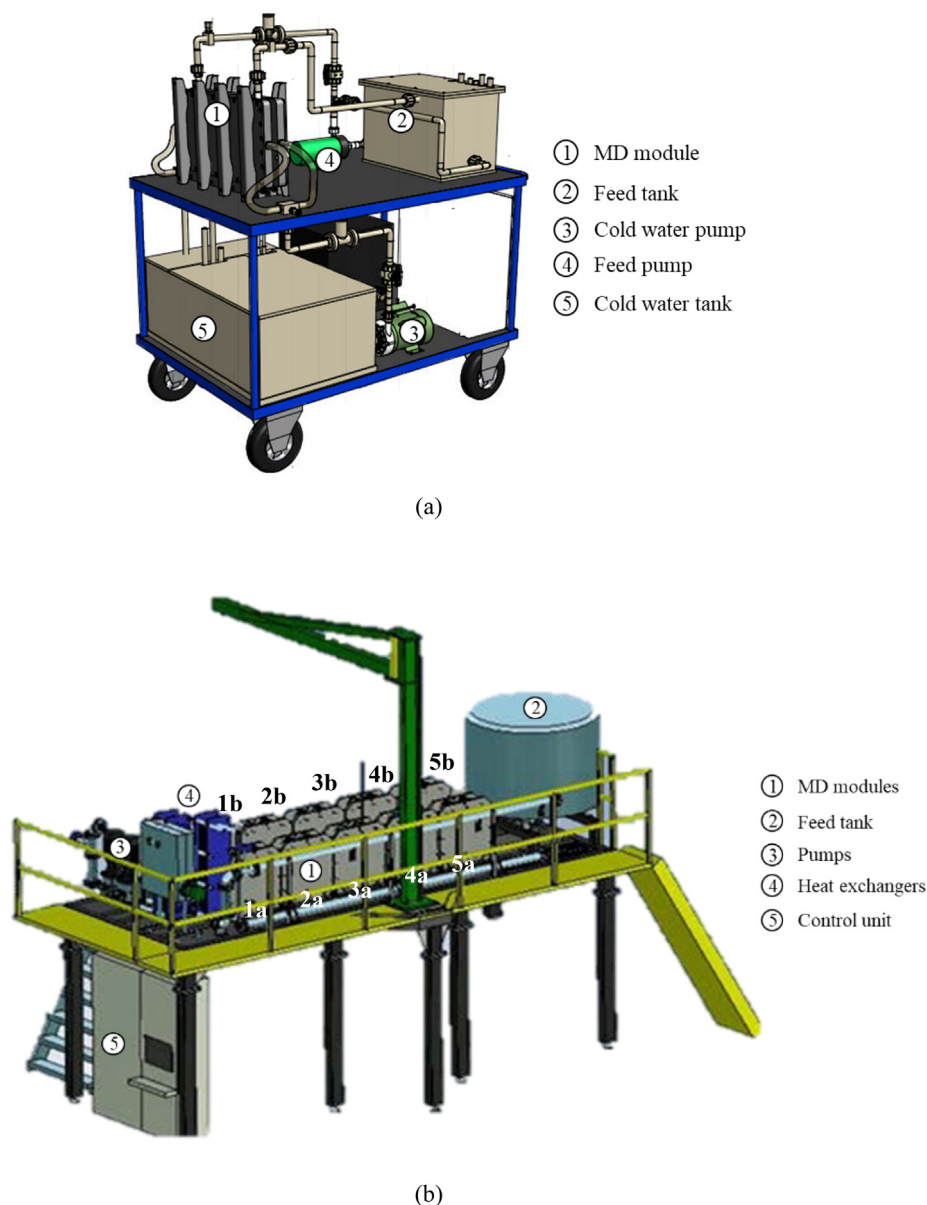


Fig. 2. Membrane distillation test units a) Xzero lab prototype b) Xzero pilot scale unit.

with carbon dioxide that cannot be removed by RO filters. Therefore, degassing step is necessary ahead which also reduces the ionic load on the electro-deionization filters. The electro-deionized boiler make up quality water (conductivity  $< 0.1 \mu\text{S}/\text{cm}$ ) is then finally sent to the boiler feed water tanks.

While the above water treatment system has proven to be satisfactory, there are a few operation and maintenance issues that are worthy of note. Biofouling has been observed in the UF modules, and in some cases was so severe as to reduce the throughput by a factor of four and increased maintenance frequency from two cleanings per year to one cleaning per week. The issue was solved by sodium hypochlorite (NaOCl) dosing in the buffer tanks. Scaling has been observed in the RO membranes, which causes some concern as to the long-term maintenance requirements for this unit. Furthermore, the separation efficiency of certain pollutants is no longer sufficiently high owing to tightened environmental regulations. In this case the system has difficulty in managing acceptable levels of mercury (Hg), boron (B), and ammonia ( $\text{NH}_3$ ), pointing to the need for additional investments in water treatment technology.

The alternative configuration considers replacing the RO based

system downstream of the shaking screens with an MD system (see Fig. 1). For simplicity the MD system is assumed to have a recovery ratio of 100% (the actual RO-based system normally achieves 90% recovery of pure water).

### 3. Methodology

#### 3.1. Experimental setup

Fig. 2 presents the experimental facilities considered in this study: 1) Xzero laboratory prototype; and 2) Xzero pilot plant. Both facilities employ air gap MD modules with polytetrafluoroethylene (PTFE) membranes (back support material, polypropylene (PP)), however, the scale and other features differ.

The laboratory prototype is installed at Xzero AB and has a nominal capacity of 1–2 L/h. This facility consists of a single cassette placed between two condensation plates. Membranes are attached to both sides of the polyethylene (PE) cassette using beam clamping and PTFE sealing. The size of the MD module is 55 cm wide, 40 cm high and 16 cm thick with active membrane area per module of  $0.194 \text{ m}^2$ . The

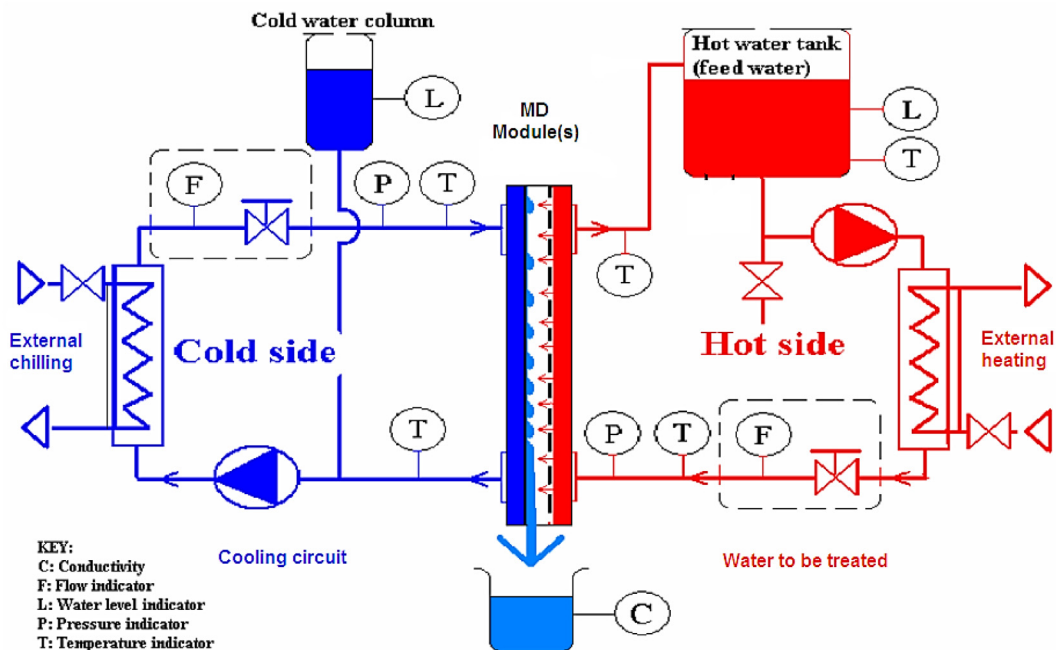


Fig. 3. Schematic Flow Diagram of AGMD separation process.

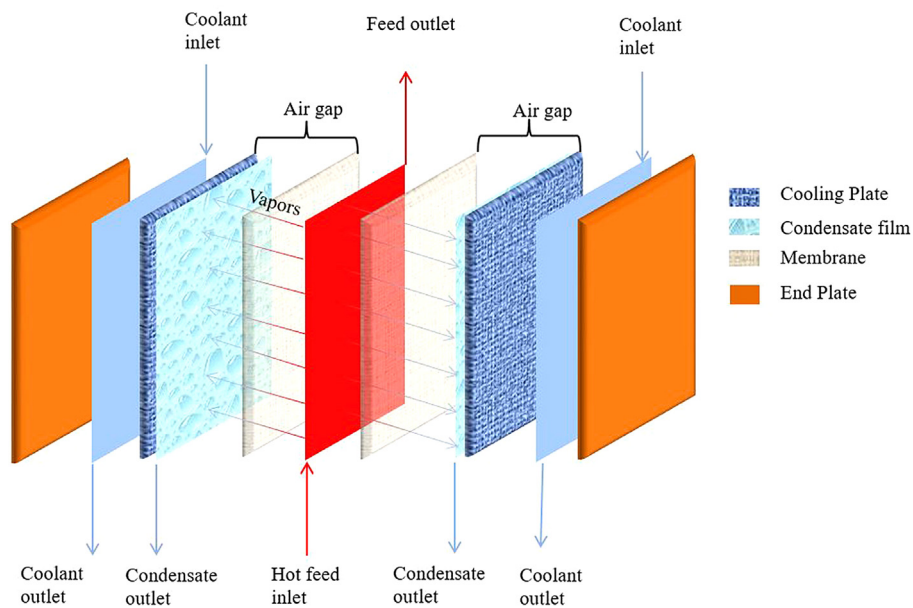


Fig. 4. Exploded diagram of AGMD cassette.

**Table 1**  
Experimental conditions of phase A testing.

Parameters	Specifications
Feed sample volume (L)	10
Feed temperature (°C)	70
Coolant temperature (°C)	18
Feed flowrate (L/min)	4.9
Coolant water flowrate (L/min)	6.8
Permeate sample Size (L)	1

**Table 2**  
Experimental conditions of phase B testing.

Parameters	Specifications
Feed sample volume (m <sup>3</sup> )	1
Feed temperature (°C)	55, 70, 80
Coolant temperature (°C)	15, 25, 50
Feed and coolant flowrate (L/min)	10
Permeate sample Size (L)	1

PTFE membranes were supplied by Donaldson® having following characteristics: thickness 254 μm; pore size 0.2 μm; porosity 80%; and liquid entry pressure of 345 kPa. The material used for condensation

plates in the module is aluminum coated with polyvinylidene fluoride (PVDF). A 30 L PVDF tank installed with PTFE coated immersion heater (capacity: 2 kW) is utilized for feed storage and an 80 L PP tank integrated with R1134a chiller (capacity: 1.8 kW) is employed for cold

**Table 3**  
Separation efficiency of MD module (Xzero lab prototype).

	Units	After Shaking screens				Before RO			RO treated permeate	Limits
		S1	D1-A	S1*	D1-A*	S2	D2-A	S2*	D2-A*	
Ca	mg/l	< 0.2	< 0.2	< 0.2	< 0.2	< 0.2	< 0.2	< 0.2	< 0.2	< 0.2
Fe	mg/l	< 0.01	< 0.01	< 0.01	< 0.01	< 0.01	< 0.01	0.0184	< 0.01	< 0.01
K	mg/l	0.61	< 0.4	0.623	< 0.4	0.46	< 0.4	0.745	< 0.4	< 0.4
Mg	mg/l	< 0.2	< 0.2	< 0.2	< 0.2	< 0.2	< 0.2	< 0.2	< 0.2	< 0.2
Na	mg/l	109	< 0.5	112	< 0.5	102	< 0.5	102	< 0.5	10.6
Al	µg/l	< 10	< 10	19.9	< 10	< 10	< 10	41.5	< 10	< 10
As	µg/l	< 0.5	< 0.5	< 0.5	< 0.5	< 0.5	< 0.5	< 0.5	< 0.5	< 0.5
Ba	µg/l	1.71	< 1	1.34	< 1	1.07	< 1	1.2	< 1	< 1
Cd	µg/l	1.46	0.19	1.48	0.64	1.05	0.1	1.28	0.28	0.12
Co	µg/l	< 0.2	< 0.2	< 0.2	< 0.2	< 0.2	< 0.2	< 0.2	< 0.2	< 0.2
Cr	µg/l	< 0.9	< 0.9	< 0.9	< 0.9	< 0.9	< 0.9	< 0.9	< 0.9	< 0.9
Cu	µg/l	9.03	< 1	10.1	< 1	8.04	< 1	30.4	< 1	1.03
Hg	µg/l	0.27	< 0.02	0.412	< 0.02	0.21	< 0.02	1.03	< 0.02	0.17
Mn	µg/l	< 0.9	< 0.9	< 0.9	< 0.9	< 0.9	< 0.9	< 0.9	< 0.9	< 0.9
Ni	µg/l	< 0.6	< 0.6	2.22	< 0.6	< 0.6	< 0.6	5.72	0.86	< 0.6
Pb	µg/l	37.6	0.84	36.9	4.4	25.7	0.58	28.2	2.54	1.66
Zn	µg/l	229	< 4	204	< 4	147	< 4	145	< 4	4.58
Mo	µg/l	< 0.5	< 0.5	< 0.5	< 0.5	< 0.5	< 0.5	0.605	< 0.5	< 0.5
V	µg/l	< 0.2	< 0.2	< 0.2	< 0.2	< 0.2	< 0.2	< 0.2	< 0.2	< 0.2
Tl	µg/l	< 0.1	< 0.1	< 0.1	< 0.1	< 0.1	< 0.1	< 0.1	< 0.1	< 0.1
Total Hardness	°dH	< 0.1	< 0.1	< 0.1	< 0.1	< 0.1	< 0.1	< 0.1	< 0.1	< 0.1
COD <sub>Cr</sub>	mg/l	< 5.0	< 5.0	7	< 5.0	< 5.0	6	< 5.0	< 5.0	< 5.0
TDS	mg/l	273	20	544	< 10	257	20	754	< 10	37
Ammonium	mg/l	35.8	23	35.3	< 0.05	28.8	15	28.4	< 0.05	3.32
Ammoniacal-nitrogen	mg/l	27.8	18	27.4	< 0.04	22.4	12	22.1	< 0.04	2.58
TOC	mg/l	0.21	0.29	0.93	< 0.50	1.1	0.58	2.06	0.62	0.1
Chloride	mg/l	26	< 0.1	26	1.2	23	0.11	24	0.65	1.2
Sulfate	mg/l	91	0.39	390	3.4	74	0.62	540	2.8	2.8
Conductivity	mS/m	66.1	12	187	0.6	58.9	6.3	300	0.41	6.5
Turbidity	FNU	0.34	< 0.2	< 0.2	< 0.2	< 0.2	0.11	< 0.2	< 0.2	< 0.2
pH		8.3	8.6	2.58	4.88	8.3	9.2	2.24	5.22	7.6
Alkalinity	mg HCO <sub>3</sub> /l	220	72	< 2.4	< 2.4	210	49	< 2.4	< 2.4	32

'<' indicates a value below the respective detection limit of the measuring equipment.

water storage. Iwaki Sverige AB pumps are connected to the system for recirculating feed and cold side fluids. Temperatures are measured with pT100 sensors and flow rates are controlled by FIP FlowX3 (paddle-wheel flow sensors f3.00/f6.30). All sensors and alarms are monitored and controlled by a Crouzet logic unit.

The Xzero pilot facility was constructed in a joint project between KTH Royal Institute of Technology and IVL Swedish Environmental Institute and is currently installed at Hammarby Sjöstadverket. This facility consists of five cascades which are connected in parallel where each cascade has two MD modules in series. Each MD module is 63 cm wide, 73 cm high and 17.5 cm thick, and contains ten cassettes. The way of membrane attachment to these cassettes is thermal welding and O ring sealing. The active membrane area per module is 2.3 m<sup>2</sup> and the collective capacity of this pilot facility is 100–200 L/h of permeate production. The used membrane was supplied by Gore® having following characteristics: thickness 200 µm; pore size 0.2 µm; porosity 80%; and liquid entry pressure of 368 kPa. The air gap of 1 mm is maintained between the membranes and condensation plates. These condensation plates are made up of PP. A 900 L steel tank having 24 kW of immersion heaters was used for hot feed storage. The system is also connected with DH return line to fulfill the additional requirement of thermal energy. Grundfos AB pumps are employed for recirculating hot feed and cold water across the MD modules. The temperatures are measured with pT100 and flow rates are controlled by rotameters. Temperature and flow sensors and alarms are monitored and controlled by Citect Runtime SCADA and Melsort.

Fig. 3 presents the schematic flow diagram of AGMD process used in both aforementioned facilities, where the system is divided into feed side (hot side) and coolant side (cold side). The hot feed is introduced to MD modules where water vapor is transported through the hydrophobic membrane owing to an imposed vapor pressure difference across the membrane. The water vapor is condensed in the air gap while

transferring energy to the coolant in the cooling plates. The condensate (clean permeate) is gravity fed to the bottom of the modules. Various sensors are installed to ensure proper operation and fulfill safety measures. Fig. 4 shows the exploded view of AGMD cassette for visual description of the process.

### 3.2. Experimental procedure

The present study was completed in two phases (A and B). In phase A, the Xzero lab prototype was employed while in phase B, the Xzero pilot plant was considered during the experiments. Section 3.2.1 provides the further details about the experimental methods. Separation efficiency of both modules at different conditions has been determined. Reconcentration and parametric studies were also performed to evaluate the complete potential of the MD based flue gas condensate treatment process.

#### 3.2.1. Separation efficiency

For phase A, actual flue gas condensate samples (~60 L) from Högdalen CHP plant were collected in October 2018 from three different points: shaking screens outlet from SP1 (S1); RO inlet from SP2 (S2); and raw boiler water tank inlet from SP3 (S3). Note that S3 is the resulting RO permeate with S2 as the feed. In this phase, the Xzero lab prototype was used for experimental runs for two cases: no pretreatment; and acid neutralization pretreatment, achieved by adding 0.9 mL/L of 40% concentrated sulfuric acid in order to lower the pH. The adopted pretreatment step was taken from Noor et al. [21,22]. After pretreatment, the samples S1 and S2 are denoted as S1\* and S2\*. Technical performance and separation efficiency of the Xzero AGMD lab prototype was determined. Table 1 presents the operating parameters and conditions for experimental runs in phase A.

In phase B of testing, a 3 m<sup>3</sup> flue gas condensate sample was

**Table 4**  
Separation efficiency of MD module 5a (Xzero Pilot Plant).

	Units	S4	S4*	D4a*	D4b*	D4c*	D4d*	D4e*	D4f*	D4g*	D4h*	S3	Limits
Ca	mg/l	0.12	8.5	< 0.050	< 0.050	< 0.050	0.19	< 0.050	< 0.050	< 0.050	< 0.050	< 0.2	
Fe	mg/l	< 0.0050	2	< 0.0050	< 0.0050	< 0.0050	< 0.0050	0.0051	< 0.0050	< 0.0050	0.018	< 0.01	
K	mg/l	0.74	0.98	< 0.10	< 0.10	< 0.10	< 0.10	< 0.10	< 0.10	< 0.10	< 0.10	< 0.4	
Mg	mg/l	< 0.10	0.61	< 0.10	< 0.10	< 0.10	< 0.10	< 0.10	< 0.10	< 0.10	< 0.10	< 0.2	
Na	mg/l	56	51	0.12	< 0.10	0.14	0.18	0.15	0.15	< 0.10	0.15	10.6	
Al	µg/l	< 10	83	< 10	< 10	< 10	< 10	< 10	11	< 10	< 10	< 10	
As	µg/l	< 0.2	1.2	< 0.2	< 0.2	< 0.2	< 0.2	< 0.2	< 0.2	< 0.2	< 0.2	< 0.5	5
Ba	µg/l	2.1	11	< 1	< 1	< 1	< 1	< 1	< 1	< 1	< 1	< 1	
Cd	µg/l	3.2	2.5	0.39	0.36	0.33	0.43	0.38	0.6	0.1	0.68	0.12	0.5
Co	µg/l	< 0.05	0.88	< 0.05	< 0.05	< 0.05	0.12	0.057	< 0.05	< 0.05	0.07	< 0.2	5
Cr	µg/l	< 0.5	170	< 0.5	< 0.5	< 0.5	< 0.5	0.65	< 0.5	< 0.5	3.2	< 0.9	5
Cu	µg/l	13	160	< 0.5	0.58	< 0.5	< 0.5	< 0.5	< 0.5	< 0.5	0.84	1.03	15
Hg	µg/l	0.32	0.25	< 0.1	< 0.1	< 0.1	< 0.1	< 0.1	< 0.1	< 0.1	< 0.1	0.17	0.25
Mn	µg/l	0.63	21	< 0.5	< 0.5	< 0.5	< 0.5	< 0.5	< 0.5	< 0.5	0.74	< 0.9	
Ni	µg/l	< 0.5	180	< 0.5	< 0.5	< 0.5	0.55	1.3	< 0.5	< 0.5	1.4	< 0.6	5
Pb	µg/l	32	55	2.2	2	1.5	2.1	2.1	4.2	< 0.5	4.9	1.66	5
Zn	µg/l	290	1700	3.1	3.4	14	14	23	9.8	< 2	26	4.58	25
Mo	µg/l	< 0.2	1.7	< 0.2	0.48	< 0.2	0.3	< 0.2	< 0.2	< 0.2	< 0.2	< 0.5	
V	µg/l	< 0.2	1	< 0.2	< 0.2	< 0.2	< 0.2	< 0.2	< 0.2	< 0.2	< 0.2	< 0.2	
Tl	µg/l	< 0.1	< 0.1	< 0.1	< 0.1	< 0.1	< 0.1	< 0.1	< 0.1	< 0.1	< 0.1	< 0.1	5
Ti	µg/l	< 0.5	< 50	< 50	< 50	< 50	< 50	< 50	< 50	< 50	< 50	< 50	
Total Hardness	°dH	< 0.15	1.3	< 0.15	< 0.15	< 0.15	< 0.15	< 0.15	< 0.15	< 0.15	< 0.15	< 0.1	
COD <sub>Cr</sub>	mg/l	< 20	< 20	< 20	< 20	< 20	< 20	< 20	< 20	< 20	< 20	< 5.0	
TDS	g/l	0.61	0.55	< 0.02	< 0.02	< 0.02	< 0.02	< 0.02	< 0.02	< 0.02	< 0.02	37	
Ammonium	mg/l	22	27	0.023	< 0.026	< 0.010	0.035	0.071	0.017	0.026	0.055	3.32	7.5
Ammoniacal-nitrogen	mg/l	17	21	0.018	< 0.020	< 0.010	0.027	0.055	0.013	0.02	0.043	2.58	
TOC	mg/l	< 2.0	< 2.0	< 2.0	< 2.0	< 2.0	< 2.0	< 2.0	< 2.0	< 2.0	< 2.0	0.1	
Chloride	mg/l	21	22	< 0.10	< 0.10	< 0.10	< 0.10	< 0.10	< 0.10	< 0.10	< 0.10	1.2	
Sulfate	mg/l	23	450	< 1.0	< 1.0	< 1.0	< 1.0	< 1.0	< 1.0	< 1.0	< 1.0	2.8	
Conductivity	mS/m	38	250	< 2.0	< 2.0	< 2.0	< 2.0	< 2.0	< 2.0	< 2.0	< 2.0	6.5	
Turbidity	FNU	0.39	0.19	< 0.10	< 0.10	< 0.10	0.15	0.17	0.11	0.1	0.17	< 0.2	
pH		7.5	2.4	4.6	4.8	5.4	5	4.9	5.2	5.2	5	7.6	
Alkalinity	mg HCO <sub>3</sub> /l	150	< 2.0	< 2.0	< 2.0	< 2.0	< 2.0	< 2.0	< 2.0	< 2.0	< 2.0	32	

Flue gas condensate sample without neutralization : S4; neutralized feed sample : S4\*; Permeate sample at T<sub>f</sub> = 55 and T<sub>c</sub> = 15: D4a\* ; Permeate sample at T<sub>f</sub> = 55 and T<sub>c</sub> = 25: D4b\* ; Permeate sample at T<sub>f</sub> = 70 and T<sub>c</sub> = 15: D4c\* ; Permeate sample at T<sub>f</sub> = 70 and T<sub>c</sub> = 25: D4d\* ; Permeate sample at T<sub>f</sub> = 70 and T<sub>c</sub> = 50: D4e\* ; Permeate sample at T<sub>f</sub> = 80 and T<sub>c</sub> = 15: D4f\* ; Permeate sample at T<sub>f</sub> = 80 and T<sub>c</sub> = 25 : D4g\* ; Permeate sample at T<sub>f</sub> = 80 and T<sub>c</sub> = 50: D4h\* ; RO permeate before raw boiler water tank : S3. ‘ < ’ indicates a value below the respective detection limit of the measuring equipment. Note that samples of MD treated permeate and RO treated permeates are sent to different external laboratories. Therefore, different detection limits can be observed.

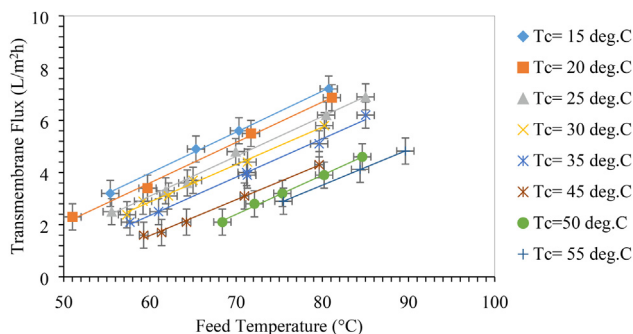


**Fig. 5.** Effect of MD feed and cold-water temperatures on transmembrane flux considering constant MD feed and cold-water flow rate of 20 L/min.

collected at the shaking screens outlet from SP1 (S4, similar to S1) in March 2019. Pretreatment was achieved by neutralizing with 37% H<sub>2</sub>SO<sub>4</sub> (1 mL/L) to achieve the desired pH level (this feed is denoted as S4\*). A total of 1 m<sup>3</sup> of the S4\* feed was pumped through a 10 µm filter prior to filling the feed tank of the MD pilot facility. Owing to the limitation of available equipment, only module 5a was used. Table 2 presents the operating parameters and conditions for experimental runs in phase B.

Feed, concentrate and permeate samples (each 1L) were collected in glass bottles and sent to independent laboratories for determination of metals concentration (Ca, Fe, K, Mg, Na, Al, As, Ba, Cd, Co, Cr, Cu, Hg, Mn, Ni, Pb, Zn, Mo, V and Tl), pH, cation concentration (ammonium), anions concentration (chloride and sulfate), total hardness, chemical

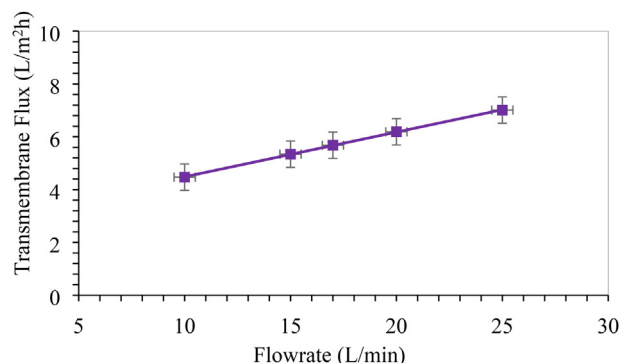


**Fig. 6.** Effect of MD feed and cold-water flowrates on transmembrane flux considering constant MD feed temperature of 80 °C and cold-water flow rate of 25 °C.

oxygen demand (COD<sub>Cr</sub>), total dissolved solids (TDS), total organic carbon (TOC), turbidity, alkalinity and conductivity. The methods used for external analyses are provided in appendix 1 (Table A3).

### 3.2.2. Permeate yield and energy demand

Apart from determining the separation efficiency in phase B of testing, a parametric study has also been performed while considering different feed and coolant temperatures and flowrates. For understanding the effect of these parameters on the performance of MD pilot plant when neutralized flue gas condensate sample was considered as feed, ranges of feed temperatures (50–90 °C, in increments of 5 °C),

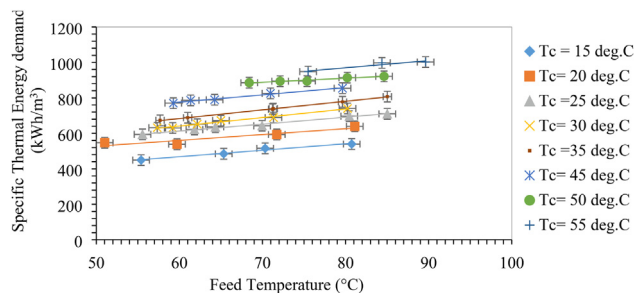


Fig. 7. Effect of MD feed and cold-water temperatures on specific thermal energy demand considering constant MD feed and cold-water flow rate of 20 L/min.

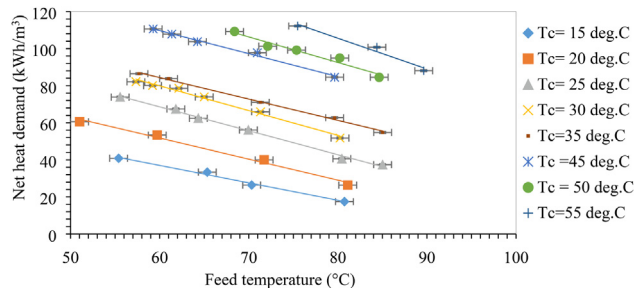


Fig. 8. Effect of MD feed and cold-water temperatures on net heat demand considering constant MD feed and cold-water flow rate of 20 L/min.

coolant temperatures (15–55 °C, in increments of 5 °C), and feed and coolant flowrates (10–25 L/min, in increments of 5 L/min) were used. The permeate flow rate was measured at different conditions and transmembrane flux was calculated using Equation (1).

Table 5

Product yield at each step of flue gas condensate reconcentration study.

Stages	Elapsed time (h)	DH return line temperature (°C)	Feed temperature (°C)	Coolant temperature (°C)	Product yield (L)
1	19.2	55.1	50.2	20.1	430
2	20.0	53.2	51.1	20.5	450
3	22.1	56.3	50.5	20.2	500
4	23.4	54.4	50.6	21.3	480
5	21.1	56.3	52.9	21.4	440

$$F_m = \frac{\dot{V}_p}{A_m} \tag{1}$$

where  $F_m$  represents transmembrane flux,  $\dot{V}_p$  presents permeate volumetric flow rate and  $A_m$  is membrane active area.

Moreover, MD feed outlet and coolant outlet temperatures were monitored and used for calculating thermal energy demand. Equations (2) and (3) define the total specific and net specific thermal energy demands as functions of flowrates and inlet/outlet temperatures:

$$\dot{Q}_h = \frac{\dot{m}_h c_p (T_{h,i} - T_{h,o})}{\dot{V}_p} \tag{2}$$

$$\dot{Q}_n = \frac{\dot{m}_h c_p (T_{h,i} - T_{h,o}) - \dot{m}_c c_p (T_{c,o} - T_{c,i})}{\dot{V}_p} \tag{3}$$

where  $\dot{Q}_h$  and  $\dot{Q}_n$  are total specific and net specific thermal energy demands, and  $\dot{m}_h$  and  $\dot{m}_c$  are the mass flow rates of hot and cold streams.  $T_{h,i}$  and  $T_{h,o}$  are hot feed inlet and outlet temperatures while cold water inlet and outlet temperatures are denoted by  $T_{c,i}$  and  $T_{c,o}$ . The specific heat of water is termed as  $c_p$  (4180 J/kg K). It should be noted that the contribution of permeate to energy balances in the numerator of Equations (2) and (3) has been neglected.

Moreover, specific electrical energy demand for operating pumps

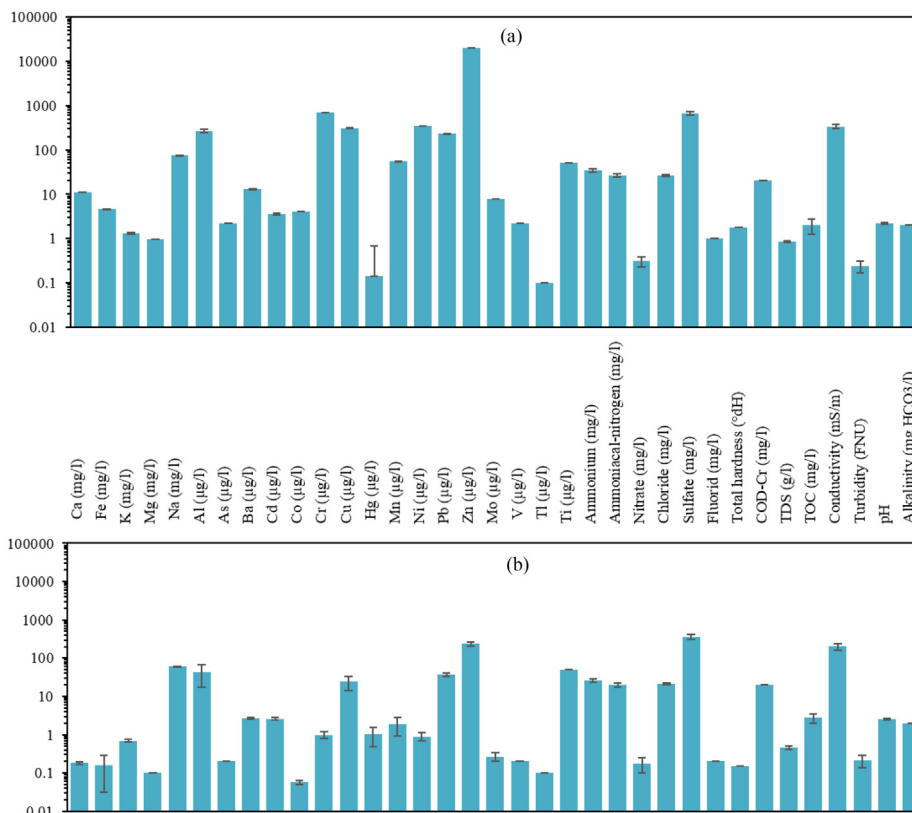


Fig. 9. Physico-chemical analyses of a) initial flue gas condensate feed and b) makeup flue gas condensate feed for reconcentration study.

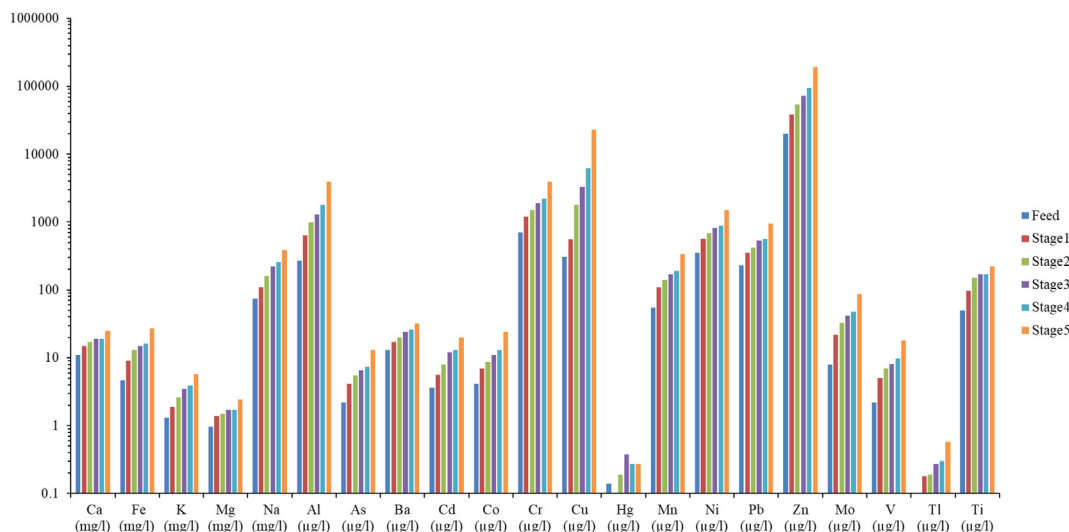


Fig. 10. Concentration levels of metals during concentrating flue gas condensate.

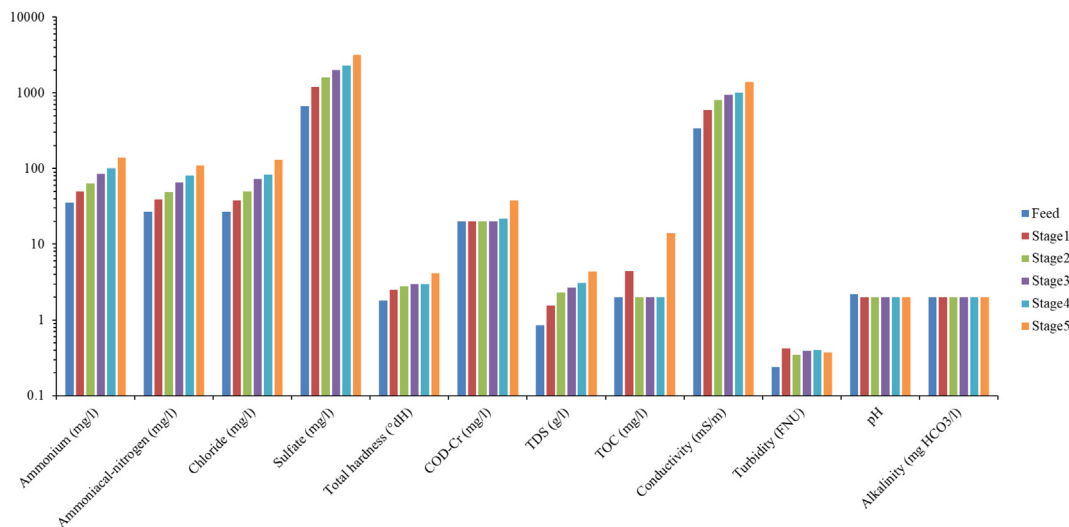


Fig. 11. Levels of water quality parameters during concentrating flue gas condensate.

was determined using Equation (4) while considering the flowrates and pressure drop across the modules.

$$\dot{Q}_e = \frac{\dot{V} \Delta P}{\eta \dot{V}_p} \quad (4)$$

where  $\dot{Q}_e$  is specific electrical energy demand,  $\Delta P$  shows pressure drop across the modules,  $\eta$  represents pump efficiency and  $\dot{V}$  is volumetric flowrate of related stream.

### 3.2.3. Reconcentration study

The reconcentration study is also performed during phase B of testing using the Xzero pilot plant. This study is considered to replicate/simulate the long-term operation of aforementioned pilot plant. The purpose is to investigate the MD performance stability at different concentration levels and to examine the potential of achieving high recovery ratios for the available pilot scale MD system. Here total feed volume of 2.5 m<sup>3</sup> was employed, and feed temperature was fixed at 50 °C while the coolant temperature was maintained at 18 °C; feed and coolant flowrates were each 50 L/min. In this case, the chosen thermal energy resource was the DH return line and a total of four modules (2a, 3a, 4a and 5a) have been used. The feed was reconcentrated for a total of 105 h and the reconcentration runs were completed in five stages.

(Tests were conducted during weekdays, thus necessitating daily start-ups and shut-downs.) At each stage, when the volume of feed reached a minimum level for maintaining adequate pump suction head, the feed tank was refilled with additional neutralized flue gas condensate sample. Samples were collected and analyzed in the manner described in section 3.2.1.

## 4. Results and discussions

### 4.1. Separation efficiency

In phase A of testing, when comparing the three samples S1, S2 and S3 (collected from different sampling points including SP1, SP2 and SP3, as shown in Fig. 1), the analysis shows that the concentration of some metals i.e., K, Na, Ba, Cu, Pb and Zn shows wide variation depending upon their sample quality, as expected. The concentration of ions (cation and anions) is higher in samples as compared to metals concentration except for Na. The levels of total hardness (< 0.1 ppm) and COD<sub>Cr</sub> (< 5 ppm) are approximately similar in all three samples. Some other important quality parameters of the samples are also determined including conductivity (6.5–66.1 µS/cm), turbidity (0.2–0.34 NTU), alkalinity (32–220 mg HCO<sub>3</sub>/l), TDS (37–273 ppm), TOC

**Table 6**  
Permeate quality of MD module 5a and 2a (Xzero Pilot Plant) during reconcentration studies at each stage.

Units	Sample from conc. Tank before each step					Permeate from module 5a					Permeate from module 2a					RO treated permeate	
	Stage1	Stage2	Stage3	Stage4	Stage5	Stage1	Stage2	Stage3	Stage4	Stage5	Stage1	Stage2	Stage3	Stage4	Stage5	S3	S5
	Ca	11	9.7	9.1	9.4	11	< 0.05	< 0.05	< 0.05	< 0.05	< 0.05	< 0.05	< 0.05	< 0.05	< 0.05	< 0.05	< 0.05
Fe	4.6	7	7.4	8.7	11	0.0083	0.0086	0.0081	0.0085	0.0093	< 0.005	< 0.005	< 0.005	< 0.005	< 0.005	< 0.005	< 0.01
K	1.3	1.5	1.7	2	2.6	< 0.1	< 0.1	< 0.1	< 0.1	< 0.1	< 0.1	< 0.1	< 0.1	< 0.1	< 0.1	< 0.1	< 0.4
Mg	0.96	0.83	0.78	0.87	0.99	< 0.1	< 0.1	< 0.1	< 0.1	< 0.1	< 0.1	< 0.1	< 0.1	< 0.1	< 0.1	< 0.1	< 0.2
Na	74	93	110	140	180	< 0.1	< 0.1	< 0.1	< 0.1	< 0.1	< 0.1	< 0.1	< 0.1	< 0.1	< 0.1	< 0.1	10.6
Al	270	390	550	920	1200	< 10	< 10	< 10	< 10	< 10	< 10	< 10	< 10	< 10	< 10	< 10	< 10
As	2.2	2.7	3.1	3.5	4.3	< 0.2	< 0.2	< 0.2	< 0.2	< 0.2	< 0.2	< 0.2	< 0.2	< 0.2	< 0.2	< 0.2	< 0.5
Ba	13	10	12	13	15	< 1	< 1	< 1	< 1	< 1	< 1	< 1	< 1	< 1	< 1	< 1	< 1
Cd	3.6	4.7	5.9	7	8.7	0.85	0.65	< 0.1	< 0.1	0.26	0.73	< 0.1	< 0.1	< 0.1	0.27	0.12	< 0.1
Co	4.1	4.4	5	6.3	7.7	< 0.05	< 0.05	< 0.05	< 0.05	< 0.05	< 0.05	< 0.05	< 0.05	< 0.05	< 0.05	< 0.05	< 0.2
Cr	700	770	860	1100	1300	0.79	0.89	0.95	1.1	4.6	< 0.5	< 0.5	< 0.5	< 0.5	< 0.5	0.68	< 0.9
Cu	310	370	1100	2600	4100	< 0.5	0.68	2.3	2.5	2.8	< 0.5	< 0.5	0.61	0.72	2.4	1.03	< 0.9
Hg	0.14	< 0.1	0.16	< 0.1	< 0.1	< 0.1	< 0.1	< 0.1	< 0.1	0.2	< 0.1	< 0.1	< 0.1	< 0.1	0.24	0.17	< 0.1
Mn	55	80	82	100	130	< 0.5	< 0.5	< 0.5	< 0.5	< 0.5	< 0.5	< 0.5	< 0.5	< 0.5	< 0.5	< 0.5	< 0.9
Ni	350	360	380	450	540	< 0.5	< 0.5	< 0.5	< 0.5	2.1	< 0.5	< 0.5	< 0.5	< 0.5	0.55	< 0.6	< 0.6
Pb	230	230	250	300	370	< 0.5	< 0.5	< 0.5	< 0.5	< 0.5	< 0.5	< 0.5	< 0.5	< 0.5	< 0.5	1.66	< 0.6
Zn	20,000	25,000	31,000	46,000	57,000	22	31	43	43	50	7.6	10	6.1	4.5	20	4.58	< 0.5
Mo	7.9	15	19	23	29	< 0.2	< 0.2	< 0.2	< 0.2	< 0.2	< 0.2	< 0.2	< 0.2	< 0.2	< 0.2	< 0.2	< 0.5
V	2.2	3.5	3.9	4.9	6.1	< 0.2	< 0.2	< 0.2	< 0.2	< 0.2	< 0.2	< 0.2	< 0.2	< 0.2	< 0.2	< 0.2	< 0.2
Tl	< 0.1	< 0.1	0.12	0.16	0.19	< 0.1	< 0.1	< 0.1	< 0.1	< 0.1	< 0.1	< 0.1	< 0.1	< 0.1	< 0.1	< 0.1	< 0.1
Ti	< 50	79	83	91	100	< 50	< 50	< 50	< 50	< 50	< 50	< 50	< 50	< 50	< 50	< 50	< 0.1
Total hardness	1.8	1.5	1.5	1.5	1.8	< 0.15	< 0.15	< 0.15	< 0.15	< 0.15	< 0.15	< 0.15	< 0.15	< 0.15	< 0.15	< 0.15	< 0.1
COD <sub>Cr</sub>	< 20	< 20	< 20	< 20	< 20	< 20	< 20	< 20	< 20	< 20	< 20	< 20	< 20	< 20	< 20	< 20	< 5.0
TDS	0.85	1.32	1.18	1.65	2.09	< 0.2	< 0.2	< 0.2	< 0.2	< 0.2	< 0.2	< 0.2	< 0.2	< 0.2	< 0.2	< 0.2	37
Ammonium	35	40	48	60	72	0.045	0.044	0.051	0.071	0.22	< 0.01	< 0.01	< 0.01	< 0.01	< 0.01	0.022	3.32
Ammoniacal-nitrogen	27	31	37	47	56	0.035	0.034	0.04	0.055	0.17	< 0.01	< 0.01	< 0.01	< 0.01	< 0.01	0.017	2.58
Nitrate	0.31	< 0.1	< 0.1	0.11	0.13	< 0.1	< 0.1	< 0.1	< 0.1	< 0.1	< 0.1	< 0.1	< 0.1	< 0.1	< 0.1	< 0.1	< 0.1
TOC	< 2	< 2	< 2	< 2	< 2	< 2	< 2	< 2	< 2	< 2	< 2	< 2	< 2	< 2	< 2	< 2	0.1
Chloride	27	30	38	46	57	0.21	0.26	0.43	0.64	0.78	0.19	0.22	0.31	0.57	0.76	1.2	1.2
Sulfate	670	970	1000	1300	1600	< 1	1.4	1.4	2.2	5	< 1	< 1	< 1	< 1	1.7	2.8	2.8
Fluorid	1	0.89	0.96	0.92	0.93	< 0.2	< 0.2	< 0.2	< 0.2	< 0.2	< 0.2	< 0.2	< 0.2	< 0.2	< 0.2	< 0.2	< 0.2
Conductivity	340	520	530	620	750	< 2	< 2	< 2	< 2	< 2	< 2	< 2	< 2	< 2	< 2	< 2	6.5
Turbidity	0.24	0.33	0.22	0.31	0.39	< 0.1	< 0.1	< 0.1	< 0.1	< 0.1	0.14	< 0.1	< 0.1	< 0.1	< 0.1	< 0.1	< 0.2
pH	2.2	2	2	2	2	5	4.7	4.6	4.6	4.1	5.7	5.3	5.3	5.2	5	7.6	7.6
Alkalinity	< 2	< 2	< 2	< 2	< 2	< 2	< 2	< 2	< 2	< 2	< 2	< 2	< 2	< 2	< 2	< 2	< 2

'<' indicates a value below the respective detection limit of the measuring equipment. Note that samples of MD treated permeate and RO treated permeates are sent to different external laboratories. Therefore, different detection limits can be observed.

**Table 7**

Process economy of industrial scale MD system for water recovery from flue gas condensate in municipal solid waste fired cogeneration plants.

Economic Parameters	Option 1	Option 2
CAPEX, M\$	12.7	12.7
Annual CAPEX, M\$	1.1	1.1
Annual heat cost, M\$	0	11.3
Annual OPEX, M\$	0.27	11.6
Normalized CAPEX, \$/m <sup>3</sup>	1.4	1.4
Normalized OPEX, \$/m <sup>3</sup>	0.3	14.5
Clean condensate cost, \$/m <sup>3</sup>	1.72	16

(0.1–1.1 ppm) and pH (7.6–8.3). In this phase, permeate of S1 and S2 (without pretreatment) are referred as D1-A and D2-A, and permeate of S1\* and S2\* (with neutralization) are named as D1-A\* and D2-A\*, respectively.

Considering MD permeate samples (D1-A and D2-A), among 20 selected metals only Cd and Pb were detectable in the permeates, although the concentrations were reduced by ~ 90% and ~ 98%, respectively as compared to their MD feeds. In relation to RO performance, the removal efficiency of Na, Cu, Hg, Pb and Zn was higher with MD, and for other metals the performance of MD was comparable except for Cd. However, for all metals the concentration in MD treated permeates was under the limitation for releasing to the recipient. Comparing ionic concentration in MD treated permeate samples, it was noticed that the removal efficiency of ammonium was not significantly high i.e., 35–48% due to highly volatile nature and small molecular size of ammonia. The higher concentration of ammonium ions in MD treated permeate samples might result in higher conductivity in comparison to that of RO treated permeate sample which has lower concentration of ammonium ions. This finding points to the need for pretreatment via pH adjustment. Anion removal efficiency (Cl<sup>-</sup> and SO<sub>4</sub><sup>2-</sup>) was above 99% for MD. Moreover, in MD treated permeates, the values of other water quality parameters such as total hardness, COD<sub>Cr</sub> and turbidity were similar to the relative values in the RO treated permeate (S3). Furthermore, the level of TDS in D1-A and D2-A was relatively lower than in S3. An increase in alkalinity content in permeate samples might be attributed to CO<sub>2</sub> contamination during collection.

In terms of metallic concentration, the quality of D1-A\* and D2-A\* samples was comparable to D1-A and D2-A samples, respectively and was better than RO treated permeate sample (S3); except for Cd, Ni and Pb. However the concentration of all metals in D1-A\* and D2-A\* was below regulated limits. In case of cation, ammonium concentration in D1-A\* and D2-A\* was < 0.05 ppm while for RO permeate this value was 3.32 ppm. Considering other water quality parameters such as hardness, COD<sub>Cr</sub>, TDS, conductivity and alkalinity, their values for D1-A\* and D2-A\* were found either equal to or lower than the respective values for RO treated permeate sample (S3). Since acid neutralization

was performed as pretreatment in this case, the pH of samples D1-A\* and D2-A\* was relatively low (~5). However, it is expected that the obtained pH value will not affect the downstream processes performance. The turbidity and TOC in D1-A\* and D2-A\* were in acceptable limits. The complete physico-chemical analysis was performed for MD feed and permeate samples for phase A testing as shown in Table 3.

In phase B of testing, the Xzero pilot plant has been used for evaluating the performance of flue gas condensate treatment while using flue gas condensate collected after shaking screens (S4, referred as S4\* after neutralization) at different feed and coolant temperatures and constant feed and coolant flowrates (10 L/min each). It was seen that the temperature does not have any significant effect on the quality of the permeate samples while taking into account metallic concentration. Concentrations of Ca, Fe, Na, Cr, Cu and Ni were reduced to more than 99%. Moreover, as in phase A, Na, Cu and Hg concentrations were found lower when compared to the concentrations of RO treated permeate. It was also found out that the concentration of mentioned metals in all the permeate samples were mostly below detection limits as well as under the allowable concentration except for very few outliers. Total hardness of permeate samples was also reduced up to 92% whereas conductivity reduced from 270 mS/m to 2 mS/m (greater than 99%). Moreover, ammonium, ammoniacal-nitrogen, sulfate and chloride concentrations were under allowable limits and their removal efficiency was more than 99.5% (which was higher in comparison to the observed efficiency in RO based treatment). The pH of the MD permeates was between 4.6 and 5.4 which can be normalized to 7 when mixed with city water. Further, values of other water quality parameters including COD<sub>Cr</sub>, TDS, TOC and alkalinity were below detection limits. Additionally, turbidity and conductivity of MD treated permeates were lower than that of RO treated permeate (S3). The complete physico-chemical analysis of MD feed, concentrate and permeate samples is shown in Table 4.

#### 4.2. Permeate yield and energy demand

In phase B of testing, the effect of feed and coolant temperatures and flowrates on permeate flux and thermal energy demand were determined. Fig. 5 shows that permeate flux varied between 1.6 and 7.2 L/m<sup>2</sup>h for MD feed and coolant flowrate of 20 L/min depending upon the feed and coolant temperatures and temperature difference between feed and coolant streams. As expected, it was observed that elevated feed temperatures and lower coolant temperatures were associated with relatively higher transmembrane flux. Moreover, considering same feed to coolant temperature differences, it was also observed that higher feed temperature was responsible for slightly higher transmembrane flux.

Fig. 6 presents variation of transmembrane flux as a function of MD feed and cold-water flowrates ranging from 10 to 25 L/min for constant

**Table A1**

Flue gas condensate treatment methods in CHP plants in Sweden [25–27]

CHP Plants	Location	Boiler type	Purification methods
Värtaverket 8	Värtan (Stockholm)	Biomass (forest products) fired	MF, UF and RO
Bristaverket	Brista (Stockholm)	Biomass (wood residues) and municipal solid waste fired	MF, UF, bag filter and RO
Högdalenverket	Högdalen (Stockholm)	Municipal solid waste fired	MF, UF, bag filter and RO
Karlstad Energi	Karlstad	Biomass fired	MF, UF and RO
E. ON (Åbyverket)	Örebro	Biomass (peat and wood chips) fired	CO <sub>2</sub> degassing, MF, UF, RO, ion exchangers and ammonia removal
Möndal Energi	Möndal	Biomass fired	MF, UF, RO and EDI
Söderenergi AB	Södertälje (Stockholm)	Biomass (wood chips) fired	MF, UF, RO, EDI and ammonia removal
Umeå Energy	Umeå	Biomass fired	MF and UF
Sevab Strängnäs Energi	Strängnäs	Biomass (municipal wastes and recycled wood) fired	MF, UF, bag filter, RO, water softeners, and EDI
Karlskoga Energi	Karlskoga	Biomass (animal waste, peat, recycled paper/plastic and wood chips) fired	MF, UF, MC, RO, EDI and MB
Örtoftaverket Krafringen	Lomma	Biomass (forestry, recycled wood and peat) fired	MF, UF, MC, RO, EDI and MB
Sävenärsverket Göteborg Energi AB	Gothenburg	Biomass (forestry) fired	MF, UF, water softeners, bag filter, and RO

**Table A2**  
Features of considered AGMD units.

Features	Xzero laboratory prototype	Xzero pilot plant
Number of cascades and configuration	1	5, in parallel
Number of modules each cascade	1	2, in series
Module width × height × thickness (cm <sup>3</sup> )	55 × 40 × 16	65.5 × 70 × 21.5
Number of cassettes per module	1	10
Cassette material	PP	PP
Number of membranes each cassette	2	2
Attachment method of membrane and Cassette	Beam Clamping and PTFE sealing	Thermal welding and O ring sealing
Membrane material	PTFE	PTFE
Membrane back support material	PP	PP
Membrane manufacturer	Donaldson	Gore
Membrane active area per module (m <sup>2</sup> )	0.194	2.3
Membrane thickness (mm)	0.254	0.2
Pore size of membrane (µm)	0.2	0.2
Porosity (%)	80	80
Liquid entry pressure (kPa)	345	368
Air gap (mm)	—	1
Condensation plate material	PVDF coated Aluminum	PP
Feed water tank volume (L)	30	900
Nominal capacity (L/h permeate)	1–2	100–200
Immersion heaters capacity (kW)	2	24 (in addition DH)
Thermocouple type	pT-100	pT-100
Flow meters	FIP FlowX3	Rotameters
Pumps types	Iwaki Sverige Ab	Grundfos AB
Control system	Crouzet PLC	Citect Runtime SCADA and Melsost
Module supplier	Xzero AB	Xzero AB
Module installed	Xzero AB	Hammarby Sjöstadsverk

MD feed temperature of 80 °C and cold-water temperature of 25 °C. With increasing MD feed and cold-water flow rate, the transmembrane flux increased from 4.5 to 7 L/m<sup>2</sup>h and presented the positive linear trend. The reasons include reduced boundary layer resistance and higher bulk temperature along the feed flow path at elevated feed flowrate and higher extent of condensation at elevated coolant flowrates.

Specific thermal energy demand was mainly dependent on the extent of temperature drop of the feed stream between inlet and outlet of MD module and on respective amount of permeate produced. Fig. 7 presents the requirement of specific thermal energy for operating the pilot plant module at different feed and coolant temperatures. The thermal energy demand ranged between 450 and 1000 kWh/m<sup>3</sup> of distilled water produced when the feed temperatures were varied from 50 to 90 °C and coolant temperature increased from 15 to 55 °C (feed and coolant flowrates each set to 20 L/min). Moreover, the trends show that higher temperature drop of the feed stream at elevated feed and coolant temperatures resulted in higher thermal energy demand. It is also instructive to determine the net thermal energy demand for cases where the dissipated heat can be recovered by other processes. (For example, heat can be supplied by the DH supply line with DH return line taken as the heat sink [23]).

Fig. 8 shows that the net thermal energy demand adopted the same trend for coolant temperature rise at constant feed temperature as shown in specific thermal energy demand due to lower transmembrane flux. However, it showed the opposite trend for elevated feed temperatures compared to specific thermal energy demand at constant coolant temperature due to increased heat transfer to the cold side. The resulting net thermal energy demand was between 17.5 and 110 kWh/m<sup>3</sup>. Moreover, the specific electrical energy consumption was approximately 0.05–0.22 kWh/m<sup>3</sup> of permeate.

#### 4.3. Reconcentration study

Prior to this step, different water quality parameters along with metallic and ionic concentrations of initial feed (which was the concentrate obtained after the parametric study of phase B testing) were measured. Results of physico-chemical analyses of the initial feed and make up feed samples (S4\*) are summarized in Fig. 9a and 9b. Comparing makeup feed and initial feed, it can be seen that the makeup feed was quite diluted i.e., up to 60 times.

Table 5 shows the summary of experimental runs during the reconcentration study using 4 modules (2a, 3a, 4a and 5a) of Xzero Pilot plant. In this step, reconcentration of the feed sample was performed in five stages and recovered 92% of water from flue gas condensate sample while reducing the feed volume from 2500 L to 200 L. The findings depict that there was no significant effect of concentration variation on the flow rate of permeate but it was mainly dependent on the feed and coolant temperatures at constant feed and coolant flowrates. This reveals the stability of the product yield of the pilot scale MD system during the reconcentration study.

The results of physico-chemical analyses of flue gas condensate concentrate (from the MD feed during concentrating) is summarized in Figs. 10 and 11. It was observed that the concentration of containments in the feed was increasing while reducing the feed volume, as expected. Moreover, the other water quality factors showed the similar trend except for pH (< 2). The pH of the feed sample was decreased, the reason might be ammonia degassing and CO<sub>2</sub> dissolution in the flue gas condensate sample. Considering conductivity as another main standard, it can be seen from the outcomes that it was increased from 340 mS/m to 1400 mS/m.

Resultantly, the quality of permeate was affected to some extent due to increased concentration in the feed sample as shown in Table 6. After each stage of reconcentration study, out of 21 different metals analyzed

**Table A3**  
External analysis methods and their description.

Analysis	Description of Methods
Ca	For Determination of metals, dissolution and analysis of water samples was performed, 12 mL sample and 1.2 mL HNO <sub>3</sub> (suprapur) have treated in autoclave.
Fe	
K	
Mg	
Na	
Al	
As	
Ba	
Cd	
Co	
Cr	
Cu	
Hg	
Mn	
Ni	i. Analysis with ICP-SFMS has been done according to SS EN ISO 17294–1, 2 (Mod) and EPA method 200.8 (Mod).
Pb	ii. Analysis with ICP-AES has been done according to SS EN ISO 11,885 (Mod) and EPA Method 200.7 (Mod).
Zn	iii. Hg analysis with AFS has been done according to SS-EN ISO 17852: 2008.
Mo	
V	
Tl	
Total Hardness	Calculation of water hardness by analysis of Ca + Mg
COD <sub>Cr</sub>	For determination of COD <sub>Cr</sub> according to method based on CSN ISO 15705, CSN EN 27 888 and CSN ISO 6060.
TDS	For determination of TDS (Total Dissolved Solids), the sample is filtered through membrane filters 0.45 µm, evaporated and then dried in the heat cabinet according to method CSN 757346.
Ammonium	For determination of ammonium with spectrophotometry according to method based on CSN EN ISO 11732, CSN EN ISO13395, CSN EN 13,370 and CSN
Ammoniacal-nitrogen	EN 12506. Filtration of turbid samples is included in the method.
TOC	For determination of TOC according to DS / EN 1484: 1997.
Chloride	For determination of chloride according to DS / EN ISO 10304–1: 2009.
Sulfate	For determination of sulphate according to DS / EN ISO 10304–1: 2009.
Conductivity	For determination of conductivity according to SS-EN 27,888 Issue 1. Direct determination of the water conductivity at 25 °C. Measurement uncertainty (k = 2): ± 12% at 14.7 mS/m, ± 10% at 141 mS/m and ± 10% at 774 mS/m.
Turbidity	For determination of turbidity according to SS EN ISO 7027–1: 2016 Edition 1. Turbidity is determined nephelometrically, i.e. the light scattering in the sample is measured under given conditions. The analysis is not accredited.
pH	For determination of pH according to SS-EN ISO 10523: 2012, Issue 1. The pH at 25 ± 2° C is determined potentiometrically by pH meter and temperature compensation. Measurement uncertainty (k = 2): Rinse water: ± 0.21 at pH 6.87 and ± 0.33 at pH 11; Sewage: ± 0.21 at pH 6.87 and ± 0.33 at pH 11.
Alkalinity	Determination of alkalinity according to SS-EN ISO 9963–2 release 1. The sample is titrated with hydrochloric acid while driving carbon dioxide to the final pH 5.4. The analysis is not accredited.

in MD treated permeate, the concentrations of 14 metals (Ca, K, Mg, Na, Al, As, Ba, Co, Mn, Pb, Mo, V, Tl and Ti) were always under the detection limits. Moreover, their values were also lower than the observed values in RO treated permeate sample. The concentration of other five metals (Fe, Cr, Cu, Hg and Ni) shows that the values ranged from below detection limits to under acceptable values, and the concentrations of these metals increased marginally from stage 1 to stage 5. However, Cd and Zn concentration was above the regulatory limit during some runs, depending upon considered module while using same feedstock. It was also found that the concentrations of chloride, sulfate, ammonium and ammoniacal-nitrogen slightly increased with the increase in feed concentration. However, their levels remained under regulatory values and were lower than the observed levels in RO treated permeate sample. Nitrate and fluoride concentrations were not affected during re-concentration study. The values of other water quality parameters including total hardness, COD<sub>Cr</sub>, TDS, TOC, turbidity and alkalinity were found under the detection limits and these were also lower than the observed values in RO treated permeate samples. The pH of the permeate samples was ranged in 4.1–5.7 and showed a decreasing trend with increasing elapsed time. The reason might be the same (ammonia degassing and CO<sub>2</sub> dissolution) as mentioned above.

No scaling or fouling phenomena were observed during the re-concentration studies. However, follow-on studies would be needed to investigate this behavior in more detail.

#### 4.4. Process economy

Based on methods employed in previously reported studies [21,24], the unit cost of clean condensate was estimated while considering the

MD plant capacity of 100 m<sup>3</sup>/h (matching the amount released from Högdalen CHP facility). In this case, DH supply line was considered as heat source and DH return line was used as heat sink. Two options were analyzed: (1) DH is available at no cost and (2) DH costs 80\$/MWh (retail price). The capital expenditure (CAPEX) in both cases was similar and the key contributor was membrane modules which were accountable for 70% of total purchased equipment cost. The remaining CAPEX was responsible for heat exchangers, pumps, tanks, pipes, auxiliaries, retrofitting and insurance. The annual operating and maintenance expenditure (OPMEX) included cost of utilities (thermal and electrical energy), labor, chemicals, brine disposal and maintenance. The normalized OPMEX for proposed MD system can be as low as 0.3 \$/m<sup>3</sup> which reveals the economic superiority of the proposed MD based process compared to RO based treatment where normalized OPMEX is ~0.8 \$/m<sup>3</sup> [19]. The estimated clean condensate cost was ~1.7 \$/m<sup>3</sup> if the thermal energy is free. Table 7 presents the summary of annual expenditures and unit clean condensate cost while using MD system of capacity 100 m<sup>3</sup>/h.

#### 5. Conclusions and future directions

This study investigated the performance of membrane distillation (MD) technology for flue gas condensate cleaning in cogeneration plants, with the Högdalen facility selected for experimental campaigns at laboratory and pilot scale. The technical evaluation of MD for treatment of flue gas condensate in combination with acid neutralization proved successful in terms of high separation efficiencies of the contaminants. Obtained permeate quality was improved as compared to the existing RO based treatment system, i.e. lower heavy metals

concentrations were obtained; a higher number of elements exhibited concentrations below detection limits; lower concentrations of ammonium and ammoniacal-nitrogen were observed; and lower values of TDS, alkalinity and conductivity were obtained. During the reconcentration study, more than 92% of the water was recovered, and removal efficiency remained high with the exception of cadmium and zinc in some trials. Parametric study shows that product yield could be improved by increasing the driving forces, mainly feed temperature and feed to coolant temperature difference. The cost of clean condensate ranges from 1.7 to 16.0 \$/m<sup>3</sup> depending primarily upon the assumed cost of thermal energy in the DH supply.

Follow on studies would be needed to investigate the performance of large scale MD system installed in the cogeneration plant (for handling continuous input of flue gas condensate in order to recover pure water). Moreover, possibilities of MD-DH integration needs to be examined in detail for better understanding of system operation and how this approach can be optimized in techno-economic terms. Furthermore, employing the presented method even more efficiently requires development of MD units (including membrane and condensation plate materials and module structure). In this regard, further studies are anticipated.

## Appendix 1

Table A1. presents flue gas condensate treatment methods in some of the main CHP plants in Sweden.

Table A2. presents the characteristics of the employed equipment.

Table A3. presents the used external analysis methods and their description.

## References

- [1] I. Obernberger, Decentralized biomass combustion: state of the art and future development, *Biomass Bioenergy* 14 (1998) 33–56, [https://doi.org/10.1016/S0961-9534\(97\)00034-2](https://doi.org/10.1016/S0961-9534(97)00034-2).
- [2] S. Zhao, S. Yan, D.K. Wang, Y. Wei, H. Qi, T. Wu, P.H.M. Feron, Simultaneous heat and water recovery from flue gas by membrane condensation: Experimental investigation, *Appl. Therm. Eng.* 113 (2017) 843–850, <https://doi.org/10.1016/J.APPLTHERMALENG.2016.11.101>.
- [3] S. Hermansson, F. Lind, H. Thunman, On-line monitoring of fuel moisture-content in biomass-fired furnaces by measuring relative humidity of the flue gases, *Chem. Eng. Res. Des.* 89 (2011) 2470–2476, <https://doi.org/10.1016/J.CHERD.2011.03.018>.
- [4] M. Hellman, Handbook – Water Treatment for Energy Producing Plants, Energiforsk, Stockholm, 2015, Report No. 2015:113, ISBN 978-91-7673-113-0, <https://docplayer.se/9783119-Handbok-i-vattenkemi-for-energianlaggningar.html>.
- [5] N.P. Cheremisinoff, Chapter 9 – Membrane Separation Technologies, Handbook of Water and Wastewater Treatment Technologies, Butterworth-Heinemann, 2002, pp. 335–371, , <https://doi.org/10.1016/B978-075067498-0/50012-7>.
- [6] J. Uotila, Heat Recovery and Environmental Impacts of Flue Gas Condensing, Thesis, Aalto University, 2015.
- [7] K. Kylhammar, Comparative Evaluation of Membrane Based Condensate Treatment Systems for Biomass-fired CHP Plants, Thesis, Lund University, 2018.
- [8] M. Khayet, T. Matsuura, Membrane Distillation: Principles and Applications, Elsevier, 2011, <https://books.google.fi/books?id=5yzHdm8vOqMC>.
- [9] K.W. Lawson, D.R. Lloyd, Membrane distillation, *J. Memb. Sci.* 124 (1997) 1–25, [https://doi.org/10.1016/S0376-7388\(96\)00236-0](https://doi.org/10.1016/S0376-7388(96)00236-0).
- [10] A. Alkudhri, N. Darwish, N. Hilal, Membrane distillation: A comprehensive review, *Desalination* 287 (2012) 2–18, <https://doi.org/10.1016/j.desal.2011.08.027>.
- [11] A.M. Alkhalibi, N. Lior, Membrane-distillation desalination: Status and potential, *Desalination* 171 (2005) 111–131, <https://doi.org/10.1016/j.desal.2004.03.024>.
- [12] A. Deshmukh, C. Boo, V. Karanikola, S. Lin, A.P. Straub, T. Tong, D.M. Warsinger, M. Elimelech, Membrane distillation at the water-energy nexus: limits, opportunities, and challenges, *Energy Environ. Sci.* (2018), <https://doi.org/10.1039/C8EE00291F>.
- [13] T. Tong, M. Elimelech, The Global Rise of Zero Liquid Discharge for Wastewater Management: Drivers, Technologies, and Future Directions, *Environ. Sci. Technol.* 50 (2016) 6846–6855, <https://doi.org/10.1021/acs.est.6b01000>.
- [14] L. Chuanfeng, A. Martin, Membrane Distillation and Applications for Water Purification in Thermal Cogeneration-A Pre-Study, Varmeforsk Service AB, Sweden, 2005 ISSN 0282-3772 <https://www.osti.gov/etdweb/servlets/purl/20588016>.
- [15] A. Kullab, A. Martin, Membrane distillation and applications for water purification in thermal cogeneration plants, *Sep. Purif. Technol.* 76 (2011) 231–237, <https://doi.org/10.1016/j.seppur.2010.09.028>.
- [16] A. Kullab, Desalination using Membrane Distillation: Experimental and Numerical Study, Thesis, KTH Royal Institute of Technology (2011).
- [17] U. Fortkamp, H. Royen, M. Klingspor, Ö. Ekengren, A. Martin, D.M. Woldemariam, Membrane Distillation Pilot Tests for Different Wastewaters, IVL Swedish Environmental Research Institute Ltd, Stockholm, 2015 Report No. B 2236 <http://www.ivl.se/download/18.7e136029152c7d48c201f3/1455531631194/B2236.pdf>.
- [18] B. Goldschmidt, L. Wiig, M. Lord, Minskning av ammoniumhalt i rökgaskondensat, Energiforsk Stockholm (2016) Report No. 2015:194, ISBN 978-91-7673-194-9, <https://energiforskmedia.blob.core.windows.net/media/21401/minskning-av-ammoniumhalt-i-rokgaskondensat-energiforskrapport-205-194.pdf>.
- [19] J. Lundgren, Personal Communication, Stockholm Exergi (2018).
- [20] Study Visit, Stockholm Exergi, 2018.
- [21] I.-. Noor, J. Coenen, A. Martin, O. Dahl, M. Åslin, Experimental investigation and techno-economic analysis of tetramethylammonium hydroxide removal from wastewater in nano-electronics manufacturing via membrane distillation, *J. Memb. Sci.* 579 (2019) 283–293, <https://doi.org/10.1016/J.MEMSCI.2019.02.067>.
- [22] I.-. Noor, J. Coenen, A. Martin, O. Dahl, Performance assessment of chemical-mechanical planarization wastewater treatment in nano-electronics industries using membrane distillation, *Sep. Purif. Technol.* 235 (2020) 116201, , <https://doi.org/10.1016/J.SEPPUR.2019.116201>.
- [23] D.M. Woldemariam, A. Kullab, A.R. Martin, District Heat-Driven Water Purification via Membrane Distillation: New Possibilities for Applications in Pharmaceutical Industries, *Ind. Eng. Chem. Res.* 56 (2017) 2540–2548, <https://doi.org/10.1021/acs.iecr.6b04740>.
- [24] I.-. Noor, A. Martin, O. Dahl, Techno-economic system analysis of membrane distillation process for treatment of chemical mechanical planarization wastewater in nano-electronics industries, *Sep. Purif. Technol.* (2020) 117013, , <https://doi.org/10.1016/j.seppur.2020.117013>.
- [25] L. Wiig, K. Lundkvist, B. Goldschmidt, H. Östfeldt, Mikrobiell Tillväxt I Rökgaskondensatreningar, Energiforsk, Stockholm, 2018 Report No. 2018:489, ISBN 978-91-7673-489-6 <https://energiforskmedia.blob.core.windows.net/media/24661/mikrobiell-tillvaxt-i-rokgaskondensatreningar-energiforskrapport-2018-489.pdf>.
- [26] Radscan Intervex Projects, (n.d.). [www.radscan.se](http://www.radscan.se) (accessed December 12, 2019).
- [27] M. Teppeler, J. Wood, P. Buzzell, Flue Gas Condensate and Energy Recovery, The McIlvaine Company, Karlskoga, 2017 IWC-08-17 [http://www.mcilvaine.com/Decision\\_Tree/subscriber/articles/Flue\\_Gas\\_Condensate\\_and\\_Energy\\_Recovery.pdf](http://www.mcilvaine.com/Decision_Tree/subscriber/articles/Flue_Gas_Condensate_and_Energy_Recovery.pdf).